

# Novel Acrylamide Assisted Polymeric Citrate Route for the Synthesis of Nanocrystalline ZrO<sub>2</sub> Powders for Dental Applications

S. Vivekanandhan<sup>\*</sup>, M. Venkateswarlu<sup>\*\*</sup>, H. R. Rawls<sup>\*\*\*</sup>, N. Satyanarayana<sup>\*</sup>

<sup>\*</sup> Department of Physics, Pondicherry University, Pondicherry- 605 014, India, nallanis2000@yahoo.com

<sup>\*\*</sup> HBL Power Systems Ltd, Hyderabad- 500 078, India,

<sup>\*\*\*</sup> University of Texas Health Science Center at San Antonio, Department of Restorative Dentistry, 7703 Floyd Curl Drive, San Antonio, TX 78229, USA

## ABSTRACT

The acrylamide assisted polymeric citrate route was investigated for the synthesis of nanocrystalline ZrO<sub>2</sub> powders, using zirconium oxychloride as the source for metal ion along with citric acid and acrylamide as chelating as well as polymerizing agents. The complete process for the synthesis of nanocrystalline ZrO<sub>2</sub> powders was monitored by TG/DTA, FTIR, XRD and TEM techniques. Thermal decomposition of the polymeric intermediate was investigated using TG/DTA analysis. Structural coordination and phase of the synthesized ZrO<sub>2</sub> powders were investigated by FTIR and XRD analysis respectively. The microstructure of the synthesized nanocrystalline ZrO<sub>2</sub> powder was identified using transmission electron microscopy, which showed ~10nm agglomerates of still finer ZrO<sub>2</sub> particles.

**Keywords:** Nanocrystalline ZrO<sub>2</sub>, Acrylamide, combustion, TG/DTA, FTIR, XRD, TEM.

## 1 INTRODUCTION

Zirconium oxide has been found to have wider range of biomedical applications than other ceramic materials, because of its high mechanical strength, fracture toughness, bio-compatibility, etc. [1-3]. Also, zirconia powders have been shown to have enhanced performance as reinforcing fillers in dental composites due their physicochemical properties [4]. Recently it is found that the zirconia based biomaterials with nanocrystalline phase exhibits an enhanced performance due to the smallest crystallite size as well as larger surface area [5]. Synthesis of nanostructured zirconia powders with desired properties (size and shape) is often difficult, since nanoscale particles agglomerate easily due to the high surface reactivity [6, 7]. In order to overcome these disadvantages, wet chemical routes, such as sol-gel, combustion, etc., have been investigated for the preparation of a wide range of nano structured metal oxides, including nanocrystalline zirconia powders [8-12].

Among the available routes, the polymeric citrate process, which is also a combustion process, has been found to be a versatile route to the synthesis of a wide range

of metal oxides with controlled morphologies [13, 16]. Basic principle of polymeric citrate process is to distribute the metal ions though out the polymeric network uniformly, which also inhibit the metal ion precipitation. Thermal decomposition of the polymeric intermediate lead to the formation of fine ceramic powders [17]. Recently, we found that addition of acrylamide to polymeric citrate enhances polymerization during the evaporation process and leads to the formation of a highly porous intermediate material. Thermal decomposition of the porous intermediate leads to the formation of non agglomerated, independent particles. Hence, in the present work, nanocrystalline ZrO<sub>2</sub> powders were prepared by the acrylamide assisted polymeric citrate route, and the complete synthesis process and the final product were investigated through TG/DTA, FTIR, XRD and TEM techniques.

## 2 EXPERIMENTAL TECHNIQUES

Fig 1 shows the schematic procedure for the synthesis of nanocrystalline ZrO<sub>2</sub> powders. Required amount of zirconium oxychloride (AR, Sd-Fine, India) was first mixed with concentrated nitric acid and boiled for 10 min. Citric acid (CA) (SQ grade, Qualigences, India) and acrylamide (ACD) (AR, Sd-Fine, India) solutions were added to the zirconium oxychloride and nitric acid mixture by keeping the total metal ions to CA ratio of 1:1 and total metal ions to ACD ratio of 1:0.5 and the resulting solutions were heated at 80°C under constant stirring. Evaporation resulted in the formation of polymeric resin. This was dried at 150°C for 24 hours and the resulting highly porous intermediate was calcined at 600°C to obtained nano crystalline ZrO<sub>2</sub> powders, which were characterized using TG/DTA, FTIR, and XRD, and TEM analysis.

Thermal behavior of the polymeric intermediate was investigated by simultaneous TG/DTA measurement using a LybSys thermal analyzer (Setaram, France). Approximately, 3mg of polymeric intermediate was heated at a rate of 10°C min<sup>-1</sup> between 30 – 600°C. All thermal studies were performed in flowing oxygen. Fourier transform infrared (FTIR) spectra were recorded using a FTIR - 8000 spectrophotometer (Shimadzu, Japan), to identify the structural coordination of as-prepared as well

as-calcined polymeric intermediate. The FTIR measurements were carried out between 400 and 4000  $\text{cm}^{-1}$  with KBr dilution. X-ray diffraction (XRD) patterns were recorded using an X-ray powder diffractometer (Rigaku, Japan), employing  $\text{Cu K}\alpha$  radiation. The volume fraction of the monoclinic phase ( $V_m$ ) was determined using the following empirical formula [18].

$$V_m = [I_m(111) + I_m(11\bar{1})] / [I_m(111) + I_m(11\bar{1}) + I_t(111)]$$

where  $I_m$  – intensities of the monoclinic peaks and  $I_t$  – Intensities of the tetragonal peaks. Microstructure of the polymeric intermediate was taken using transmission electron microscope (Jeol, Japan). The samples for TEM measurements were prepared by dispersing the polymeric intermediate powder in high purity acetone and sonicated for 2 min. Using tweezers, a carbon coated copper grid was immediately dipped into the sonicated suspension, then dried and TEM images collected.

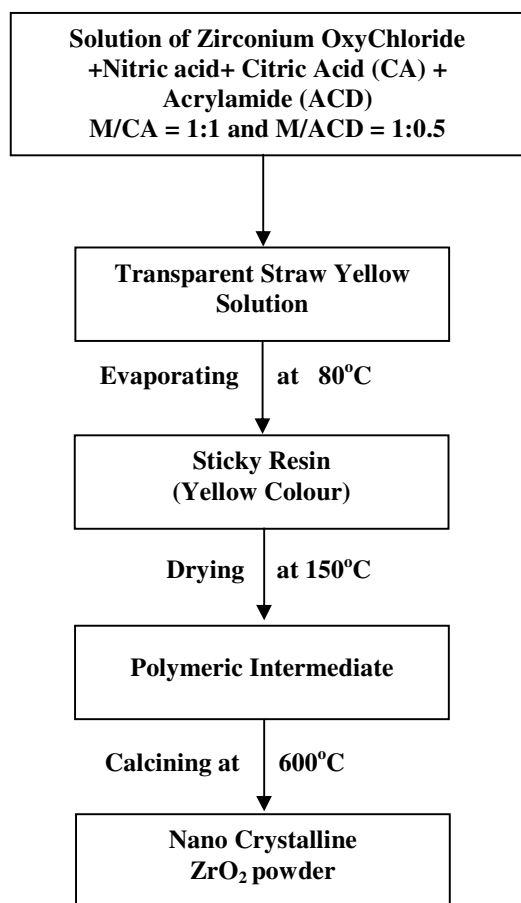


Figure 1. Schematic diagram for the synthesis of nanocrystalline  $\text{ZrO}_2$  powder by the acrylamide assisted polymeric citrate route

### 3 RESULTS AND DISCUSSION

TG/DTA thermogram of the polymeric intermediate is shown in fig 2. The observed exothermic peak with a major weight loss of ~40% in the TGA curve indicates the combustion of organic derivatives, which begins at 300°C and is complete at 575°C. Also, the observed small exothermal peak between 500 and 575 °C, may be due to the crystallization of  $\text{ZrO}_2$ . No further weight loss is observed above 575 °C, which may indicate the formation of  $\text{ZrO}_2$  structure. This is confirmed by FTIR and XRD analysis.

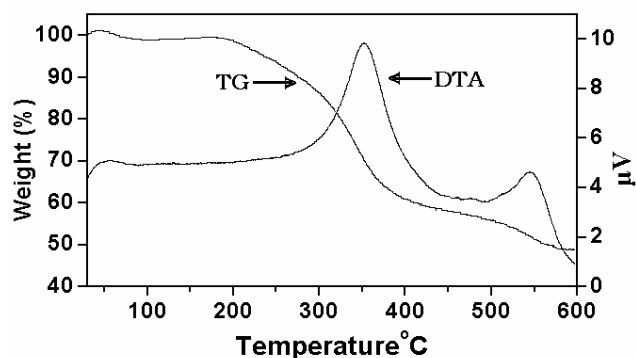


Figure 2 TG/DTA thermogram of the polymeric intermediate

Fig 3 shows the FTIR spectrum of the synthesized  $\text{ZrO}_2$  powder. The observed IR peaks at 747-755  $\text{cm}^{-1}$  and 498-502  $\text{cm}^{-1}$  are attributed to the vibration modes of the  $\text{ZrO}_3^{2-}$  group, and confirm the formation of  $\text{ZrO}_2$  [19, 20]. The observed FTIR spectrum does not show any peaks related to the organic derivatives, which confirm that complete decomposition occurred during the calcination process, as observed in the TG/DTA analysis.

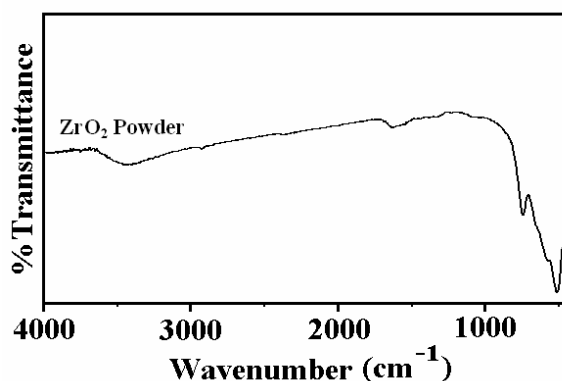


Figure 3 FTIR spectrum of synthesized  $\text{ZrO}_2$  Powder

Figure 4 shows the XRD pattern of synthesized  $ZrO_2$  powder prepared at  $600\text{ }^\circ\text{C}$ . From fig.4, the observed x-ray diffraction peaks are compared with the JCPDS data and confirm the formation of mixed phases of tetragonal (t- $ZrO_2$ ) and monoclinic (m- $ZrO_2$ ) zirconium oxides. The volume fraction was calculated using XRD data. The volume fractions obtained for the tetragonal and monoclinic phases are respectively 53.4 % and 46.6 %.

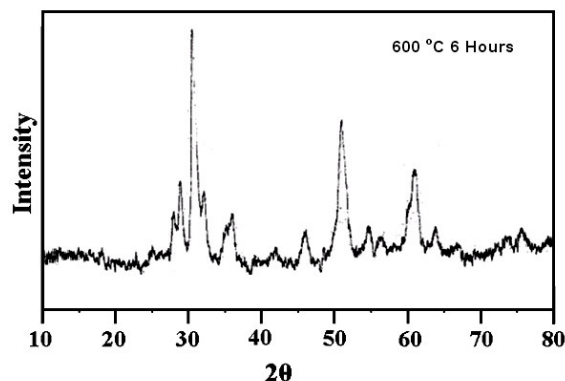


Figure 4 XRD pattern of synthesized  $ZrO_2$  Powder

Microstructure of the synthesized  $ZrO_2$  powder is identified through TEM analysis. Fig.5 shows the TEM micrographs of the synthesized  $ZrO_2$  powder. The TEM images show  $<1000\text{ nm}$  agglomerations of primary  $ZrO_2$  particles that are in the size range of  $\sim 10\text{-}20\text{ nm}$ . Synthesized  $ZrO_2$  particles are planned for use in the development of nanocomposite resin materials for dental and other biomedical applications.

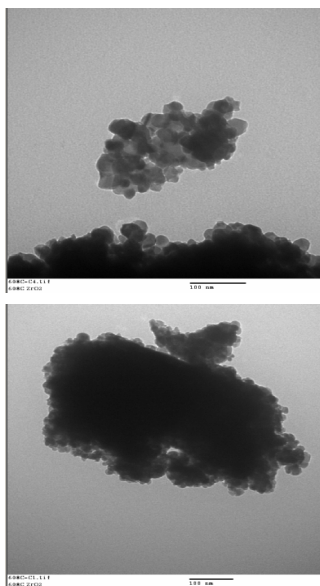


Figure 5 TEM micrographs of the nanocrystalline  $ZrO_2$  powder

## 4 CONCLUSIONS

The acrylamide-assisted polymeric citrate route is an attractive means for the synthesis of nanocrystalline  $ZrO_2$  powder. From TG/DTA, FTIR and XRD results, it is found that the organic-free nanocrystalline  $ZrO_2$  particles are formed at  $600\text{ }^\circ\text{C}$  with two different phases of tetragonal and monoclinic. Their volume fractions were calculated using XRD data found to be 53.4 % for t- $ZrO_2$  phase and 46.6% for m- $ZrO_2$  phase. Transmission electron micrographs show that the synthesized  $ZrO_2$  particles occur as agglomerates of  $\sim 1\text{-}20\text{ nm}$  primary  $ZrO_2$ .

## 5 ACKNOWLEDGEMENTS

NS gratefully acknowledges DST, CSIR and DRDO for utilizing the research facilities available from their major research projects. SV acknowledges the CSIR, Government of India, for the award of a senior research fellowship. HRR was supported NIH, National Institute for Dental and Craniofacial Research grant P01-DE11688.

## REFERENCES

- [1]. R. Srinivasan, C. R. Hubbard, O. B. Cavin and B. H. Davis, *Chem. Mater.*, 5, 27-29, (1993).
- [2]. M. Valigi, D. Gazzoli, G. Ferrarisa, E. Bemporad, *Phys. Chem. Chem. Phys.*, 5, 4974-4980, (2003).
- [3]. R. Morena, P. E. Lockwood, A. L. Evans, C. W. Fairhurst, *J. Am. Ceram. Soc.*, 69 [4], C-15-C-77, (1986).
- [4]. J. L Ferracane, *Crit. Rev. Oral Biol. Med.*, 6(4), 302-318, (1995).
- [5]. A. V. Shevchenko, E. V. Dudnik, A. K. Ruban, V. P. Red'ko, V. M. Vereschaka, and L. M. Lopato, *Powder Metall. Met. Ceram.*, Vol. 41, Nos. 11-12, 558-563, (2002).
- [6]. M. Kakihana, S. Kato, M. Yashima, M. Yoshimura, *J. Alloys Compd.*, 280, 125-130, (1998).
- [7]. X. Feng, M. Z. Hu, *Encyclopedia of Nanoscience and Nano technology*, Edited by H. S. Nalwa, American Scientific Publishers, Vol. 1, 687-726 (2004).
- [8]. L.J. Fu, H. Liu, C. Li, Y.P. Wu, E. Rahm, R. Holze, H.Q. Wu, *Prog. Mater. Sci.*, 50 881-928 (2005).
- [9]. L.W. Tai, P.A. Lessing, *J. Mater. Res.* 7 (2), 502-510, (2002).
- [10]. S. Ammar, A. Helfen, N. Jouini, F. Fievet, L. Rosenman, F. Villain, P. Molinie, M. Danot, *J. Mater. Chem.*, 11, 186-192 (2001).
- [11]. S. Bucella, P. Riello, B.F. Scremin, P. Calvelli, R. Polloni, A. Speghini, M. Bettinelli, A. Benedetti, *Optical Materials*, 27, 249-255, (2004).
- [12]. M. Pechini, US Patent No. 3 330 697, July 11, 1967.
- [13]. Y. W. Zhang, Z. G. Yan, F. H. Liao, C. S. Liao, C. H. Yan, *Mater. Res. Bull.*, 39, 1763-1777, (2004).

- [14]. A. Majid, J. Tunney, S. Argue, D. Wang, M. Post, J. Margeson, *J. Alloys Compd.*, 398, 48–54, (2005).
- [15]. Rajesh Ganesan, S. Vivekanandhan, T. Gnanasekaran, G. Periaswami, Raman S. Srinivasa, *J. Nucl. Mater.* 325, 134–140, (2004).
- [16]. T. Mahata, G. Das, R. K. Mishra, B. P. Sharma, *J. Alloys Compd.*, 391, 129–135, (2005).
- [17]. S.W. Kwon, S.B. Park, G. Seo, S.T. Hwang, *J. Nucl. Mater.*, 257, 172-179, (1998).
- [18]. S. G. Chen, Y. S. Yin, D. P. Wang, X wang, *J. Mol. Struct.*, 703, 19-23, (2004).
- [19]. G. Socrates, *Infrared and Raman Characteristic Group Frequencies*, John Wiley and Sons: New York, 2001.
- [20]. A. Sreekumaran Nair, Renjis T. Tom, V. Suryanarayanan, T. Pradeep, *J. Mater. Chem.*, 13, 297–300, (2003).